JOC The Journal of Organic Chemistry

Article

pubs.acs.org/joc

Acid-Activatable Michael-Type Fluorescent Probes for Thiols and for Labeling Lysosomes in Live Cells

Chun-Guang Dai,[†] Xiao-Jiao Du,[‡] and Qin-Hua Song*[,†]

[†]Department of Chemistry, University of Science and Technology of China, Hefei 230026, P. R. China

[‡]School of Life Sciences, University of Science and Technology of China, Hefei 230027, P. R. China

Supporting Information

ABSTRACT: A Michael addition is usually taken as a base-catalyzed reaction. Most fluorescent probes have been designed to detect thiols in slightly alkaline solutions (pH 7–9). The sensing reactions of almost all Michael-type fluorescent probes for thiols are faster in a high pH solution than in a low pH solution. In this work, we synthesized a series of 7-substituted 2-(quinolin-2-ylmethylene)malonic acids (QMAs, substituents: NEt_2, OH, H, Cl, or NO_2) and their ethyl esters (QMEs) as Michael-type fluorescent probes for thiols. The sensing reactions of QMAs and QMEs occur in distinct pH ranges, pH < 7 for QMAs and pH > 7 for QMEs. On the basis of experimental and theoretic studies, we have clarified the distinct pH effects on the sensing reactivity between QMAs and QMEs and demonstrated that two QMAs (NEt_2, OH) are highly sensitive and selective fluorescent probes for thiols in acidic solutions (pH < 7) and promising dyes that can label lysosomes in live cells.

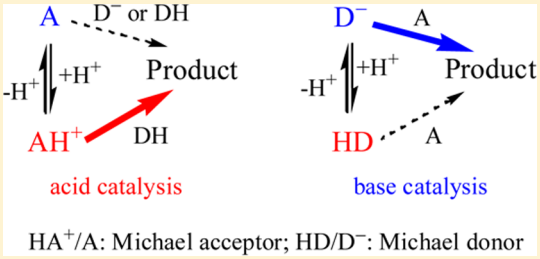

INTRODUCTION

Thiols are an important class of molecules in biological systems and chemical science. Intracellular thiols, such as cysteine (Cys), homocysteine (Hcy), and glutathione (GSH), play essential roles in many physiological processes.[1] Abnormal levels of cellular thiols are associated with many human diseases. A deficiency of Cys causes various health problems, such as retarded growth, hair depigmentation, lethargy, liver damage, muscle and fat loss, and skin lesions.[2] An elevated level of Hcy in human plasma is a risk factor for Alzheimer's disease, cardiovascular disease, neural tube defects, inflammatory bowel disease, and osteoporosis.[3] GSH is critical in maintaining redox homeostasis, which is important for the maintenance of a cellular defense against reactive oxygen species and for a number of biological processes.[4] Therefore, the detection of cellular thiols is of growing importance. Among the various detection methods, an optical approach based on synthetic colorimetric and fluorescent molecular probes has attracted increasing interest over the past decade due to their simplicity, inexpensiveness, sensitivity, and selectivity.[5]

The most important advantage of fluorescent probes is intracellular detection. A variety of colorimetric and fluorescent probes for thiols have been constructed by exploiting the strong nucleophilicity or high transition metal affinity of the thiol group, which involves specific reactions between probes and thiols, such as Michael addition,[6] nucleophilic reactions,[7] disulfide bond cleavage,[8] metal complex-displacement coordination,[9] combined multiple modes,[10,11] among others,[12,13] in the past two years. Among these probes, most cases involve the electrophilicity of probe molecules and the nucleophilicity of thiols, such as the probes via Michael addition or aromatic nucleophilic substitution (S_NAr). Because the thiolate anion RS^- is more nucleophilic than its neutral form, RSH (pK_a ~8.5), most fluorescent probes were designed to detect thiols in slightly alkaline solutions, such as pH 7.4, which is the so-called physiological condition in which the real Michael donor is the thiolate anion RS^-. In other words, these thiol probes could not work in acidic solutions owing to an insufficient concentration of RS^-.

Although a few probes that can detect thiols at low pH (<6) were reported, they are more active in alkaline solutions.[14] Recently, we developed acid-activatable colorimetric and fluorescent probes for thiols, 7-hydroxy-2-(quinolin-2-ylmethylene)malonic acids (A-OH), which can label lysosomes in live cells by a sensing reaction with biothiols.[15] The probe can detect thiols only in acidic solutions (pH <7), giving a colorimetric and fluorescent response, as shown in Scheme 1. In contrast, its ethyl ester E-OH displays a contrary pH effect on the sensing reactivity,[15,16] which can act only at pH >7, like most thiol probes reported.[6,7]

To further understand the two classes of sensing reactions, we synthesized a series of 7-substituted 2-(quinolin-2-ylmethylene)malonic acids (QMAs) and their ethyl esters (QMEs) (Chart 1), and their 7-substituents cover various groups from strong electron-donating groups (EDGs) to strong electron-withdrawing groups (EWGs). On the basis of experimental and theoretic studies on the sensing reactions of QMAs or QMEs with thiols in different pH solutions, two different sensing mechanisms have been demonstrated, that is,

Received: September 1, 2015
Published: November 6, 2015

DOI: 10.1021/acs.joc.5b02041
J. Org. Chem. 2015, 80, 12088–12099

Scheme 1. Two Kinds of Fluorescent Probes for Thiols Working in Different pH Ranges

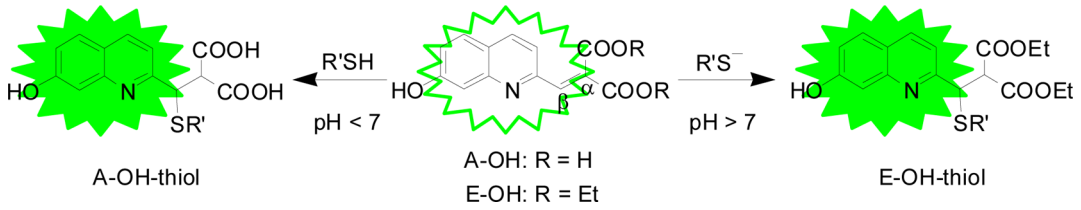

Chart 1. Chemical Structures of Two Kinds of Probes, QMAs and QMEs

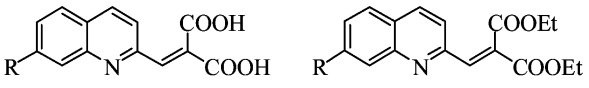

QMAs	QMEs
A-NE: R = NEt_2	E-NE: R = NEt_2
A-OH: R =OH	E-OH: R =OH
A-H: R = H	E-H: R = H
A-Cl: R = Cl	E-Cl: R = Cl
A-NO: R = NO_2	E-NO: R = NO_2

the sensing reaction of QMAs being the Michael reaction of activated QMAs with RSH in acidic solutions, and the sensing behavior of QMEs being a base-catalyzed Michael reaction with RS^- like most Michael-type probes reported.[6]

RESULTS AND DISCUSSION

1. Synthesis of QMAs and QMEs. The synthetic procedure of four QMAs and four QMEs is a two- or three-step route with 7-substituted 2-methylquinolines (**1**) as the starting material, as shown in Scheme 2. The two-step route was employed to prepare one QMA, A-NE, and four QMEs, E-NO, E-Cl, E-H, and E-NE. First, the methyl group (**1**) is oxidized with SeO_2 to form aldehyde group (**2**) in good yields (75−92%). Then, aldehydes **2** react with malonic acid or its ethyl ester via Knoevenagel condensation to give target compounds in moderate yields (50−70%) with the exception of E-NE (15%). The other three QMAs, A-NO, A-Cl, and A-H, were obtained through the hydrolysis of their esters E-NO, E-Cl, and E-H, respectively.

2. VARIOUS IONIZED STATES OF QMAS IN DIFFERENT PH SOLUTIONS

pH Effects on UV/Vis Absorption Spectra. QMAs are composed of two carboxyl groups and a pyridine ring, and there is also an *N,N*-diethylamino group for A-NE or a hydroxyl group for A-OH. The forms of these functional groups are pH dependent, such as deprotonation of carboxyl groups and the hydroxyl group, and protonation of pyridine and the amino group. Hence, QMAs can exist in several ionization forms (dicationic, cationic, neutral, anionic, dianionic, and trianionic), as shown in Scheme 3. The different ionization forms of these functional groups possess different electronic properties. Thus, various ionized-state QMAs possibly form different D-π-*A* conjugated systems, thereby, different extents of ICT processes. Correspondingly, each of the ionization forms would have different spectral properties.

Figure 1 showed UV/vis absorption spectra of A-NE in different pH solutions (pH 1−11). As shown in Figure 1, with increasing pH values of solutions, the absorption maxima occur first as red-shifts from 461 nm (pH 1.0) to 505 nm (pH 2.2) and then continuous blue-shifts to 482 nm (pH 5.6) and finally to 415 nm (pH 8.2). As the pH reaches higher than 8.2 up to 11, QMAs reveal similar absorption spectra with a maximum of ∼415 nm. The pH effects on the absorption spectra can be observed by the naked eyes from color changes of various pH solutions (pH 2−11). The photograph of A-NE in different pH solutions displays a color change from deep red to light red and then to orange (Figure S1).

Measurement of pK_a of QMAs. To measure pK_a values of QMAs, the UV/vis absorption spectra of QMAs in different pH solutions were recorded, and as an example, the absorption spectra of A-NE were shown in Figure 1. By analysis of these spectral changes with pH variation, four pK_a values of A-NE, pK_{a1}, pK_{a2}, pK_{a3}, and pK_{a4}, were obtained, and they are 1.4, 2.8, 3.4, and 7.1, respectively. As an example, plots of absorbance vs pH value for pK_a 3.4 and 7.1 are shown in insets of Figure S2.

Scheme 2. Synthetic Route of Probes QMA and QME[a]

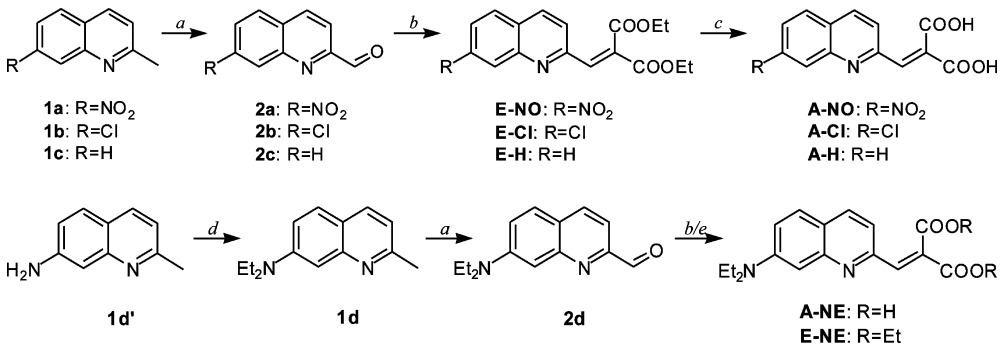

[a]Reagents and conditions: (a) SeO_2, 1,4-dioxane, 60 °C, 12 h; (b) diethyl malonate, piperidine, ethanol, 50 °C, 12 h; (c) KOH, ethanol/water, 80 °C, 2 h; (d) ethyl iodide, K_2CO_3, *N,N*-dimethylformamide, 80 °C, 7 h; and (e) malonic acid, piperidine, ethanol, 50 °C, 4 h.

DOI: 10.1021/acs.joc.5b02041
J. Org. Chem. 2015, 80, 12088−12099

Scheme 3. Various Ionization Forms of QMAs

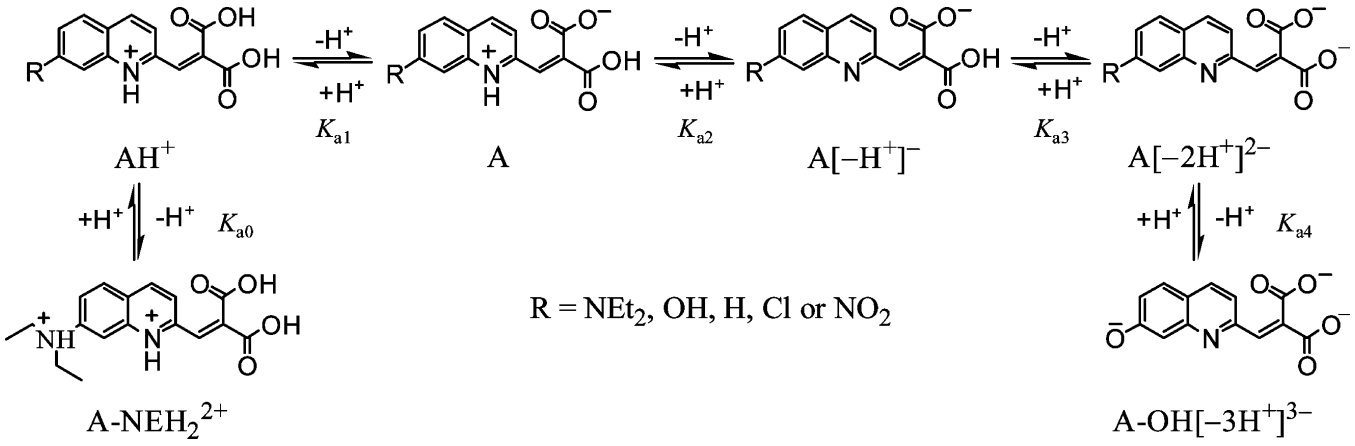

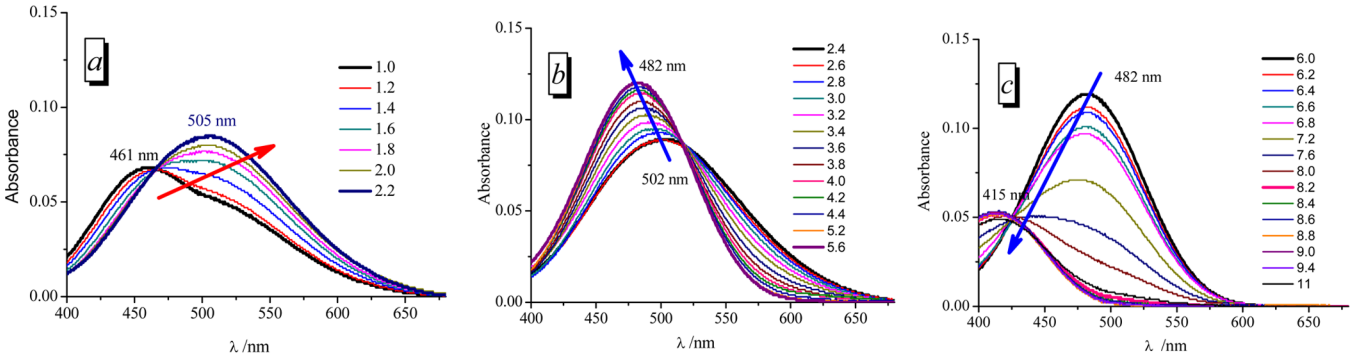

Figure 1. UV/vis absorption spectra of A-NE (20 μM) in different pH solutions ranging from pH 1 to 11.

These pK_a values are assigned to the corresponding sites of A-NE (Scheme 3). Similarly, the pK_a values of other QMAs were measured, assigned, and listed in Table 1.

Table 1. pK_a Values for Functional Groups of QMAs

QMA	pK_{a0}	pK_{a1}	pK_{a2}	pK_{a3}	pK_{a4}
A-NE	1.4	2.8	3.4	7.1	
A-OH		2.73	3.2−3.6	5.6	8.6
A-H		1.38	3.2−3.4	5.0	
A-Cl		1.36	3.2−3.4	4.6	
A-NO		1.2	2.5	3.6	

As shown in Scheme 3, there are equilibria between the ionized states of A-NE, which depend on pH values of solutions. For example, the main ionized state in the pH ranges is A-NEH_2^{2+} (pH <1.4), AH^+ (1.4−2.8), A (2.8−3.4), $A[-H^+]^-$ (3.4−7.1), or $A[-2H^+]^{2-}$ (pH >7.1), respectively. Thus, the main ionized states in several pH solutions shown in Figure S2 are A-NEH_2^{2+} (pH 1), AH^+ (pH 2.4), A (pH 3), $A[-H^+]^-$ (pH 5.6), or $A[-2H^+]^{2-}$ (pH 8.2 and 11), and their absorption maxima are 462, 503, 495, 482, and 415 nm, respectively. Other QMAs also reveal similar pH effects on their absorption spectra. Among the ionized states, $A[-2H^+]^{2-}$ possesses the shortest absorption maximum or the least conjugation system for the same QMA.

The pK_{a3} is the pH value of deprotonation of the second carboxyl group of QMAs. The deprotonation of the second carboxyl group results in a large blue-shift of the absorption maximum of QMAs. In other words, the deprotonation of the second carboxyl group would cause a large decrease in the conjugated system of QMAs. As is well-known, there is an intramolecular hydrogen bond (H-bond) between two carboxyl groups of malonic acid. Thus, the intramolecular H-bond could be responsible for a strong conjugation of the 2-methylene malonic acids, QMAs, in acidic solutions.

3. MOLECULAR CONFORMATIONS OF A-OH AND E-OH

To further understand pH effects on UV/vis absorption spectra, as a representative, we optimized the structures of various ionized-state A-OH and E-OH with the B3LYP density functional at the 6-31+G(d) level, as shown in Figure 2. There

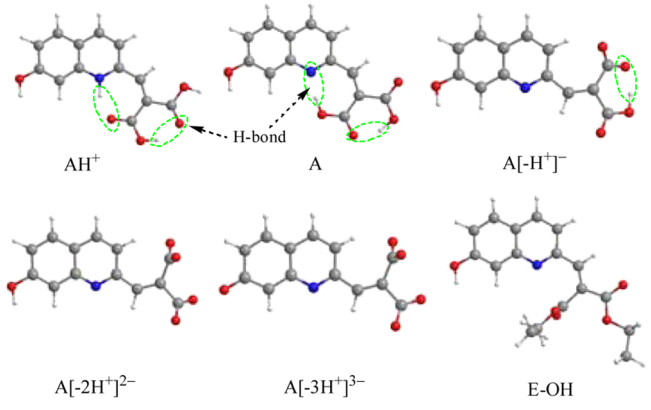

Figure 2. Optimized structures for various ionized states of A-OH and E-OH.

DOI: 10.1021/acs.joc.5b02041
J. Org. Chem. 2015, 80, 12088−12099

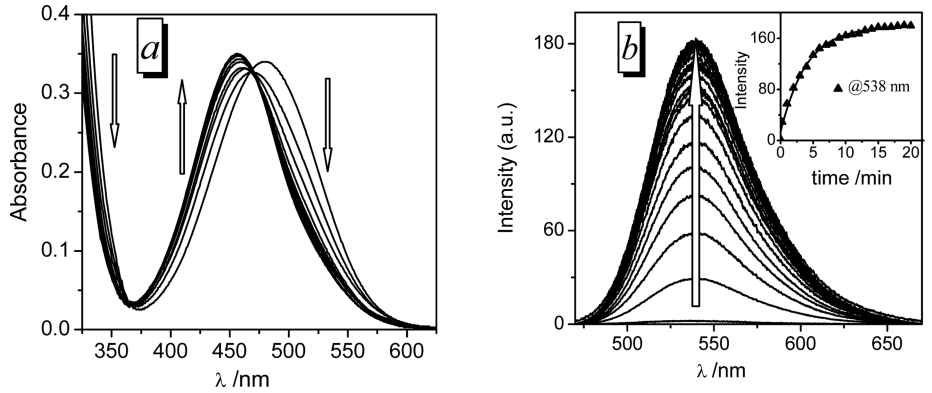

Figure 3. UV/vis absorption (a) and fluorescence (b) spectra of A-NE (20 μM, buffer solution pH 5) in the presence of 80 μM Cys recorded over 20 min. Inset: plot of fluorescence intensity at 540 nm vs reaction time; λ_{ex}= 460 nm.

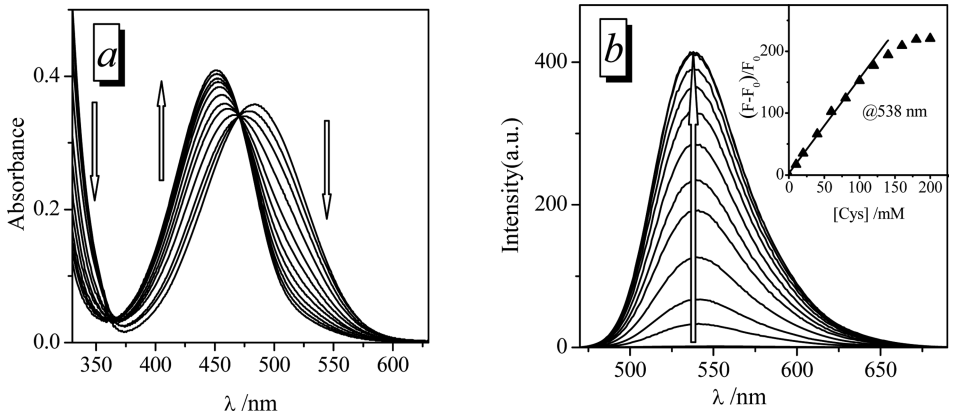

Figure 4. UV/vis absorption (a) and fluorescence (b) spectra of A-NE (20 μM) in the acidic solution (pH 5) in the presence of different concentrations of Cys ranging from 0 to 10 equiv after 30 min. Inset: fluorescence maximum as a function of Cys concentration and a straight line by linear fitting on experimental data points.

are two intramolecular H-bonds in AH^+ and A, one between two carboxyl groups (C═O···H−O) and another between the protonated nitrogen (N^+−H···O═C) and oxygen of the carbonyl group, and there is only the former H-bond in A[-H^+]$^-$. The intramolecular H-bonds cause a coplanar conformation between 2-methylene quinoline and two carboxyl groups for two ionized states, AH^+ and A, and A[-H^+]$^-$ with only one H-bond between two carboxyl groups is nearly planar. The planar conformation results in a strong conjugation between α,β-unsaturated quinoline and two carboxyl groups, which is reflected in their UV/vis absorption spectra (Figure S3). Two long-band absorption peaks at 338 and 378 nm should be assigned to the three ionized states. As the pH value is lower than 2.73, there is only one peak at 338 nm. This may be because the intramolecular H-bond between N^+−H and oxygen of the carbonyl group is destroyed due to protonation of the carbonyl group in strong acidic solutions. The ionized state, A[-H^+]$^-$, exists in slightly acidic solutions (pH 3.4−5.6). As shown at pH 5 and pH 5.6 of Figure S3, there is a long-wavelength absorption peak at 378 nm for the pH 5 solution, which decreases to be a shoulder for pH 5.6. This may be because there is no H-bond (N^+−H···O═C), leading to being noncompletely coplanar between the quinoline and 2-methylene malonic acid (Figure 2). Both A[-$2H^+$]$^{2-}$ and A[-$3H^+$]$^{3-}$ have no intramolecular H-bonds, are nonplanar molecules, and have their two carboxyl groups perpendicular to each other (Figure 2). At pH >7, there is a new weak absorption peak at 390 nm resulting from deprotonation of the 7-hydroxy group (Figure S3). For A-NE and other QMAs, a similar assignment can be obtained between UV/vis absorption spectra and various ionized states with the corresponding molecular conformation. Therefore, the intramolecular H-bond between two carboxyl groups is mainly responsible for the planar molecular conformation, which extends molecular conjugation of QMAs.

The molecular conformation of E-OH displays that one ester group is nearly perpendicular to the quinoline ring. This is in agreement with its UV/vis absorption spectrum that has two peaks of 264 and 323 nm as well as a shoulder at 368 nm (Figure S3b).

4. THE SENSING REACTION OF QMAS AND QMES TO THIOLS

Spectral Response of QMAs to Thiols. The probes A-NE and E-NE emit very weak fluorescence resulting from their effective nonradiation processes, which derive from 2-methenylene malonic acid or its ester linked to the quinoline. After the Michael addition of thiols to the α,β-double bond of A-NE and E-NE, the fluorescence of the fluorophore, *N,N*-diethylquinoline, could be restored to display "turn-on" fluorescent responses.

As expected, when 4 equiv of Cys was added to the A-NE acidic solution of DMSO/0.1 M phosphate-citric acid buffer (v/v 2/98, pH 5, 37 °C), its time-dependent UV/vis absorption spectra exhibit a ratiometric change with isosbestic points at

DOI: 10.1021/acs.joc.5b02041
J. Org. Chem. 2015, 80, 12088−12099

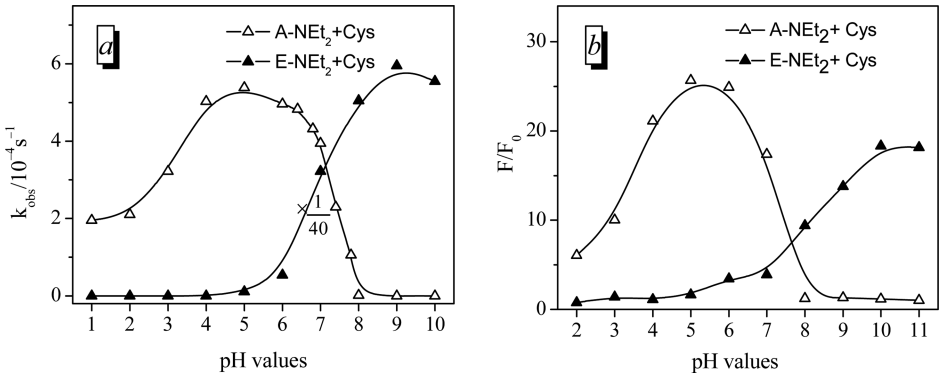

Figure 5. (a) Observed rate constants of the Michael addition of A-NE or E-NE (20 μM) with 4 equiv of Cys in various pH solutions. (b) Fluorescence increments of A-NE or E-NE after treatment with 4 equiv of Cys for 30 min as a function of pH values at room temperature.

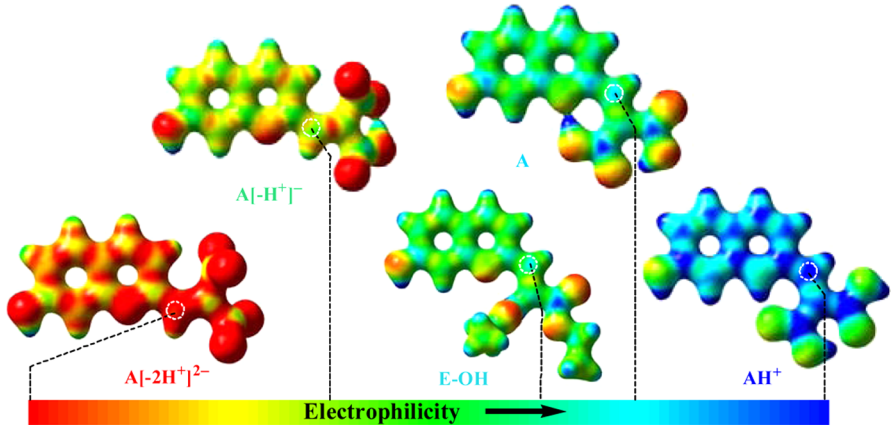

Figure 6. Electrostatic potential maps and the order of EPs at the C_β atom for various ionized states of A-OH and E-OH.

365 and 469 nm; the fluorescence gradually increases to reach a maximum in 20 min, and the enhancement of fluorescence is 96-fold (Figure 3). On the basis of the time-dependent absorption spectra, the second order rate constant of this sensing reaction was obtained as k_2 = 56 M^{-1} s^{-1} at 37 °C.

In the presence of differing amounts of Cys, the UV/vis absorption spectra of A-NE (20 μM) in the acidic solution (pH 5) also reveals a ratiometric change (Figure 4a). The fluorescence response of A-NE for different amounts of Cys was observed in the acidic solution (Figure 4b). When the concentration of Cys was increased to 10 equiv, no further increase in fluorescence intensity was observed. The fluorescence alternation displays a well-linear relationship with the concentration of Cys in the range from 0 to 100 μM. This implies that a quantitative analysis of thiols can be achieved in this concentration range. The detection limit ($3N/k$) was determined to be 45 nM, where N is the standard deviation of the intercept and k is the slope of the fitting straight line in the inset of Figure 4b.

Confirmation of the Sensing Mechanism. The sensing reaction as a Michael addition was confirmed by ^{1}H NMR spectroscopy. Upon the addition of Cys, the vinylic proton (H_α at 7.90 ppm) of A-NE disappears with the concomitant appearance of new peaks around 4.40 and 4.68 ppm, which are assigned to two protons of the adduct product A-NE−Cys (Figure S4). The high-resolution mass spectrum of the acidic solution mixture (pH 5) of A-NE and Cys showed a dominant peak at 434.1397 in accordance with the adduct of A-NE−Cys ([M − H^+]: 434.1391) (Figure S5). For another system, A-OH−Cys, the sensing reaction process has been observed by ^{1}H NMR as a Michael addition. Meanwhile, a single effective process for the Michael reaction between A-OH and Cys has been demonstrated by HPLC. Furthermore, mass spectral analysis of the resulting mixture supports the thiol-Michael addition of A-OH.[15]

pH Effects on the Sensing Reaction of A-NE and E-NE. To investigate pH effects on the sensing reactivity of A-NE, we monitored the reaction of 20 μM A-NE with 4 equiv of Cys by UV/vis absorption spectroscopy in various pH solutions ranging from pH 1 to 10. The observed rate constants (k_{obs}) were obtained from time dependent UV/vis absorption spectra, as shown in Figure 5a. The plot clearly shows that the Michael addition occurs only in acidic solution (pH <7). Moreover, two inflection points are at approximately 3.5 and 7.5, which are consistent with pK_{a2} and pK_{a3} of A-NE. This implies that A-NE as the Michael acceptor is activated as the second carboxyl group is protonated, but the protonation of the N atom of quinoline decreases the reactivity of A-NE. The highest reactivity of A-NE is at pH ∼5. These observations are similar to those[15] from A-OH, and the highest reactivity is at pH 4.6 for A-OH with Cys. These pH values are less than their pK_{a3}, i.e., 5 < 7.1 (pK_{a3} of A-NE) and 4.6 < 5.6 (pK_{a3} of A-OH). In contrast, the corresponding plot for E-NE exhibits a contrary pH effect, that is, E-NE reacts with Cys in alkaline solutions (pH >7).

Furthermore, fluorescence increments (F/F_0) of A-NE or E-NE with Cys in various pH solutions ranging from 2 to 11 were determined, as shown in Figure 5b. The fluorescence

DOI: 10.1021/acs.joc.5b02041
J. Org. Chem. 2015, 80, 12088−12099

Scheme 4. Sensing Mechanism of QMAs and QMEs

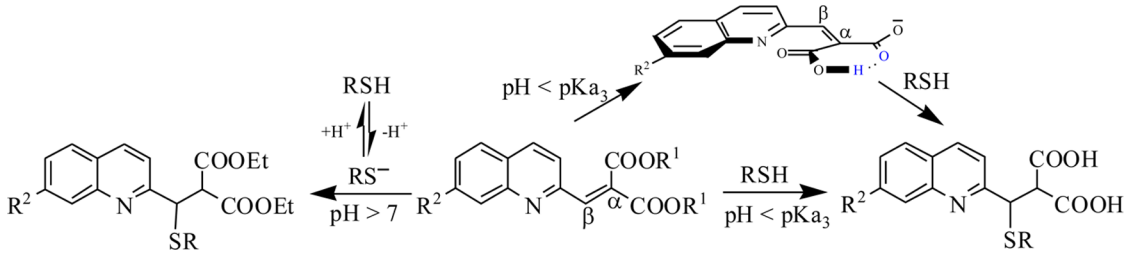

Table 2. Photophysical Properties of QMAs in A[-H$^+$]$^-$ Ionized States

QMA	pH[a]	Φ_f /10^{-3}	$^{abs}\lambda_{max}$/nm	$^{em}\lambda_{max}$/nm	Stoke's shift/nm	F/F$_0$[b]	$^{em}\lambda_{max}$[b]/nm	LOD[c]/nM
A-NE	5.0	0.23	480	535	55	100	538	45(76)
A-OH	4.6	1.6	376	515	139	21	525	71(89)
A-H	4.2	1.0	342	454	112	1.6	454	(31)
A-Cl	4.0	1.3	333	402	69	1.5	405	(38)
A-NO	3.0	*d*	284	*d*	/	/	*d*	(63)

[a]pH values of measured solutions. [b]Fluorescence increments of 20 μM QMAs with and without 80 μM Cys at 37 °C. [c]Data in parentheses from colorimetric analysis. [d]No fluorescence.

increments (F/F$_0$) in various pH solutions reveal a similar pattern to their k_{obs}. Both A-NE and E-NE emit almost no fluorescence in the whole pH range (2−11), and the reaction systems A-NE+Cys and E-NE+Cys emit strong fluorescence in the pH ranges of 3−7 and 7−11, respectively. Therefore, two probes can effectively react with thiols in different pH ranges, i.e., pH <7 for A-NE and pH >7 for E-NE, and display turn-on fluorescence responses. The sensing behavior of E-NE is similar to that of probes previously reported,[6] which have no activity at pH <7 due to thiols in neutral forms. In contrast, A-NE reacts with thiols only in acidic solutions, and its adduct A-NE−Cys gives large fluorescence increments in acidic solutions.

The pH effects described above can be observed by the naked eye from the color and fluorescence change of A-NE before and after the addition of Cys in different pH solutions (Figure S1). The acidic solutions display a color change from red to orange for solutions of pH 2−7, and no change was observed for solutions of pH 8−11. The fluorescence photos show that all solutions (pH 2−11) of neat A-NE are nonfluorescent. After the addition of Cys, green fluorescence was observed for solutions of pH 2−7, and no fluorescence was observed for solutions of pH 8−11.

Electrostatic Potential Maps of A-OH and E-OH. The electrostatic potential map (EMP) can reflect the electrophilicity at an atom of a molecule. EP maps of four ionized states of A-OH as well as E-OH are calculated with the B3LYP density functional at the 6-31+G(d) level, as shown in Figure 6. The blue color indicates a high potential, which implies that the atom in a molecule is electrophilic, and the red color represses a contrary situation. As shown in Figure 6, the cation AH$^+$ has the highest potential, and the dianion A[-2H$^+$]$^{2-}$ has the lowest potential. The electrostatic potentials of the β-carbon atom (C$_\beta$) in all ionized states are higher than those of α-carbon (C$_\alpha$). This is the reason why the Michael donor adds to the C$_\beta$ rather than the C$_\alpha$ position. The potential of C$_\beta$ of AH$^+$ is the highest and is the lowest for A[-2H$^+$]$^{2-}$ among the four ionized states. Namely, the electrophilicity of AH$^+$ is the highest and A[-2H$^+$]$^{2-}$ is the lowest. Obviously, as Michael acceptors, QMAs are acid-activatable. In acidic solutions, the intramolecular H-bond between two carboxyl groups results in a conplanar conformation with an α,β-double bond; thereby, a strong conjugation elevates C$_\beta$ electrophilicity, i.e., activating Michael acceptor QMAs (Scheme 4). The EP at C$_\beta$ of E-OH is between A and A[-H$^+$]$^-$. Thus, the electrophilic order of various ionized states of A-OH and E-OH is AH$^+$ > A > E-OH > A[-H$^+$]$^-$ > A[-2H$^+$]$^{2-}$.

Of course, the described order is not the order of the reactivity of a Michael addition. In particular, it is not the order of the reactivity of thiol-Michael reactions of QMAs and QMEs because the sensing reactions of QMAs and QMEs are in two different systems: QMAs/RSH in acidic solutions (pH < pK_{a3}) and QMEs/RS$^-$ in alkaline solutions. In fact, the rate constants of E-OH with thiols in alkaline solutions (pH 7.4) are much higher than those of all A-OH ionized states/RSH system.[15] Similar results from A-NE and E-NE were observed from Figure 5a.

The reactivity of the thiol-Michael reaction is enhanced by either elevating the C$_\beta$ electrophilicity of the Michael acceptor or forming more nucleophilic RS$^-$ in alkaline solutions. QMAs are activated by forming intramolecular H-bonds between two carboxyl groups in acidic solutions (pH < pK_{a3}), and their reactivity decreases as the H-bond deprontonates in a higher pH solution (pH > pK_{a3}). Moreover, a strong electrostatic repulsion between the low-reactivity dianion A[-2H$^+$]$^{2-}$ and RS$^-$ would suppress the reaction in alkaline solutions. Therefore, QMAs are specific fluorescence probes for thiols in acidic solutions.

5. SUBSTITUENT EFFECTS

UV/Vis Absorption and Emission Spectra of QMAs in A[-H$^+$]$^-$ Ionized States. UV/vis absorption and fluorescence spectra of five QMAs in acidic solutions (pH < pK_{a3}) were measured (Figure S6), and their photophysical properties are listed in Table 2. QMAs with a 7-substituent from an EWG to an EDG reveal bathochromic shifts for both absorption and fluorescence spectra. This indicates that the pull-push electronic character of QMAs increases as a 7-substituent from EWG to EDG. The donating ability of a 7-substituted quinoline moiety as a donor enhances with the electron-donating ability of the 7-substituent; thereby, the extent of intramolecular charge transfer (ICT) increases. The Stoke's shifts increases from A-Cl to A-OH, and the data are listed in Table 2.

DOI: 10.1021/acs.joc.5b02041
J. Org. Chem. 2015, 80, 12088−12099

The fluorescence quantum yields (Φ_F) of QMAs were determined using a fluorescein (Φ_f = 0.90 in 0.1 N NaOH)[17] solution or quinine sulfate (Φ_f = 0.54 in 0.1 N H_2SO_4)[18] as references. Fluorescence quantum yields of all five QMAs are very low, and the efficiency of A-OH is the highest (0.16%) among the five QMAs. The fluorescent increments (F/F_0) of 20 μM A-NE or A-OH in the presence of 4 equiv of Cys are 100 and 21, respectively. This shows that the two probes are very sensitive to thiols and also implies Michael adducts of both A-NE and A-OH with Cys with strong fluorescence. The fluorescence changes very little for A-H and A-Cl, and there is no fluorescence change for A-NO after the addition of Cys. Moreover, the limit of detection (LOD) for the four probes were measured at 30−70 nM and are listed in Table 2. The values of LOD show that these probes are sensitive to thiols. Although three probes, A-H, A-Cl, and A-NO, do not have a good fluorescence response to thiols, the LOD values from the colorimetric analysis are very low. In addition, the larger fluorescence maxima of adducts for A-NE (538 nm) and A-OH (525 nm) display new ICT processes in these adducts with a pyridine moiety as the electron acceptor.

pK_a of QMAs. Various pK_a values in Table 1 show that a QMA with a 7-EWG has lower pK_a values than those with a 7-EDG. For example, the pK_{a3} values are 7.1, 5.6, 5.0, 4.6, and 3.6 for five QMAs with 7-substituents of NEt_2, OH, H, Cl, and NO_2, respectively. Obviously, the QMA with a 7-EWG would increase the acidity of the functional groups.

The Reactivity of QMAs in Acidic Solutions. The second-order rate constants (k_2) of reactions of QMAs with Cys were determined at the same pH solution, such as pH 3 and pH 5 (Table 3). As shown in Table 3, the 7-substituent effect on the reactivity of QMAs displays an irregular change in the same pH solution. When the pK_{a3} of a QMA is higher than 3, the rate constant (k_2) in the pH 3 solution is higher than that in the pH 5 solution, such as A-Cl and A-NO. When the pK_{a3} was >5, two pH values are lower than it, and the k_2 value in the pH 3 solution is lower than that in the pH 5 solution, such as A-NE and A-OH.

Table 3. Substituent Effects on the Rate Constants of QMAs with Cys in Several pH Solutions[a]

QMA	pK_{a3}	k_2 (pH 3[b])	k_2 (pH 5[b])	k_2 (pH[b])
A-NE	7.1	2.9	3.8	3.8 (5)
A-OH	5.6	4.0	4.8	5.9 (4)
A-H	5.0	6.4	6.3	6.4 (3)
A-Cl	4.6	4.2	1.9	7.7 (2.5)
A-NO	3.6	3.9	0.6	9.8 (1.5)

[a]Measurements at room temperature in M^{-1} s^{-1}. [b]pH values of measured solutions.

However, the rate measurement of a QMA was performed in the solution with the pH value that is lower than its pK_{a3}, and a set of data with a regular change was obtained and shown in the last column of Table 3. The rate constants increase gradually from A-NE with a strong EDG to A-NO with a strong EWG. Namely, QMAs can be activated by a 7-EWG. However, the activation of 7-EWG was observed only in a low pH solution because the QMA with a 7-EWG has a low pK_{a3}. In other words, the electronic effect of the 7-substituent on the rate constants reveals a regular change after the formation of the intramolecular H-bond (pH < pK_{a3}), or that is to say, the activation resulting from the H-bond plays a more important role over the substituent effect.

6. SELECTIVITY AND APPLICATION IN BIOIMAGING

Selectivity. The specificity of A-NE toward thiols was investigated by the fluorescence response of A-NE in the presence of various biologically relevant analytes. Except for a little fluorescence increment for the bisulfite ion (HSO_3^-), no fluorescence enhancement was observed from A-NE solutions after the addition of 6 equiv of aniline, phenol, and other representative amino acids (Ser, Met, and Asn) (Figure 7).

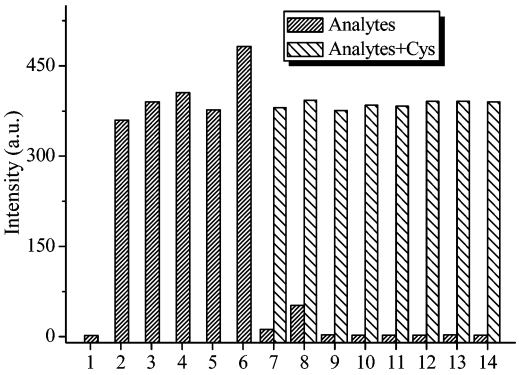

Figure 7. Fluorescence intensity (540 nm) of A-NE (20 μM) in the presence of 6 equiv of analytes recorded in the solution (DMSO/PBS, v/v 2:98, pH 5.0) after incubation for 30 min. Dense bar: 1, blank; 2, *n*-propylthiol; 3, Cys; 4, Hcy; 5, GSH; 6, methyl thioglycolate; 7, Na_2S; 8, $NaHSO_3$; 9, $Na_2S_2O_3$; 10, aniline; 11, phenol; 12, serine; 13, DL-methionine; and 14, L-asparagine. Sparse bar: addition of Cys to analyte (7−14) solutions in the presence of A-NE (20 μM).

However, under the same conditions, A-NE exhibits a larger fluorescence response to thiols (Cys, Hcy, GSH, and *n*-propylthiol) as well as to Cys under the potential competition of nucleophiles and biologically relevant analytes. These results show the specific response of A-NE to thiols.

Photostability and Cell Toxicity of Probes. The solutions of probes with and without Cys were irradiated by continuous monochromatic light from a fluorophotometer with a xenon lamp (150 W) for 120 min. Their absorption and fluorescence spectra were monitored, and no significant change in both absorption or fluorescence spectra was observed for either of the probes or their adducts with Cys, as shown in Figures S7 and S8. These results show that the photostability of the probes is excellent.

To detect thiols in living MDA-MB-231 cells, we carried out an MTT experiment to assess the cytotoxicity of the probes. In the MTT assays, MDA-MB-231 cells were dealt with probes at different concentrations from 10 to 50 μM for 24 h. The results show that the probes generate very low toxicity to cultured cells under the experimental conditions, and the cell viability is up to 87% for both A-NE and A-OH at 50 μM (Figure S9).

Cell Imaging. To test the capability of probes A-NE, A-OH, and E-NE for imaging thiols in living cells, we seeded MDA-MB-231 cells on coverslips in 24-well plates and incubated them at 37 °C. DMSO solutions of A-NE, A-OH, and E-NE were added to the wells to give a concentration of 20 μM (DMSO/culture medium, v/v 1/1000). To further investigate the lysosome localization of A-NE and A-OH, we employed a commercially available lysosomal dye (LysoTracker Red)[19] for a colocalization study; the dye can label acidic organelles, such

DOI: 10.1021/acs.joc.5b02041
J. Org. Chem. 2015, 80, 12088−12099

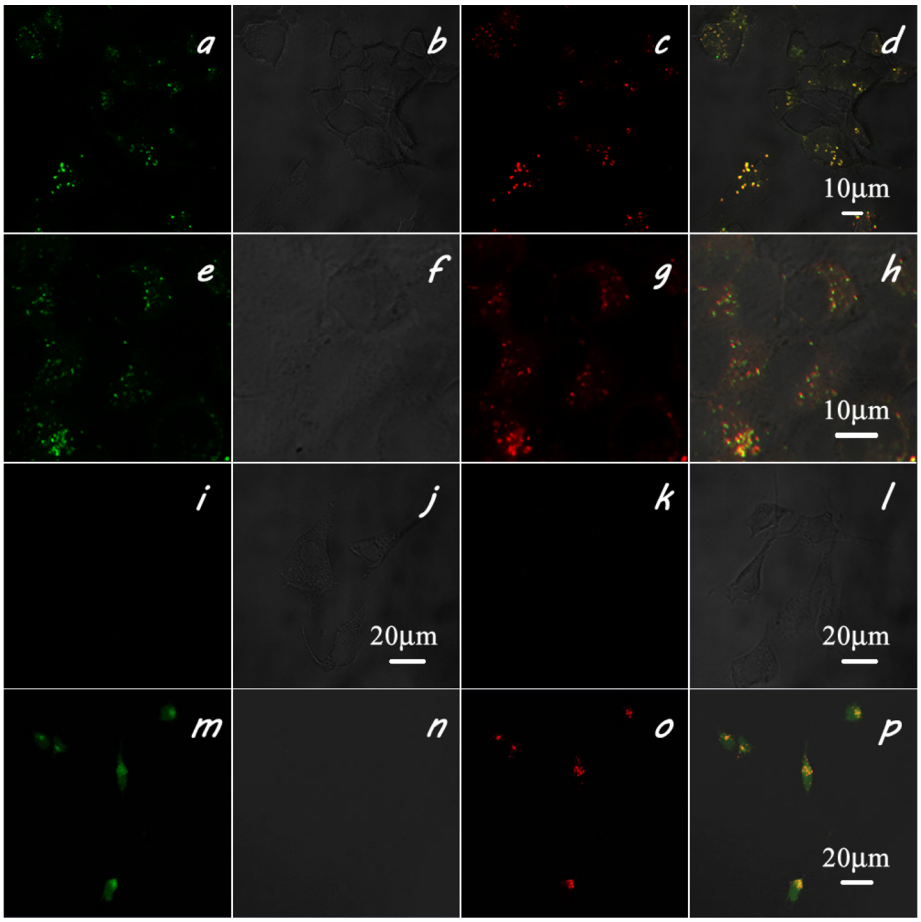

Figure 8. Confocal fluorescence images of MDA-MB 231 cells treated simultaneously with 20 μM A-NE (a–d) for 1 h, A-OH (e–h) for 3 h, or E-NE (m–p) for 1 h and 75 nM LysoTracker Red for 0.5 h: (a, e, m) green fluorescence images of A-NE, A-OH, and E-NE; (b, f, n) brightfield images; (c, g, o) red fluorescence images of LysoTracker Red; and (d, h, p) overlap images of (a–c), (e–g), and (m–o), respectively, treated simultaneously with 500 μM NEM for 1 h and A-NE (i, j) for 1 h or A-OH (k, l) for 3 h: (i, k) green fluorescence images and (j, l) brightfield images.

as lysosomes (pH ~ 5) of live cells, with red fluorescence. The probe has several important features, including high selectivity for acidic organelles and effective labeling of live cells at nanomolar concentrations. MDA-MB-231 cells were stained with A-NE or A-OH and LysoTracker Red in succession and observed under confocal fluorescence microscopy. As shown in Figure 8, the fluorescence images of A-NE (Figure 8a) and A-OH (Figure 8e) show that only partial regions of cells emit green fluorescence, which merge well with the red-channel images (Figure 8c and g) for LysoTracker Red dye (Figure 8d and h), and the overlap coefficients are 0.90 (Figure S10). The colocalization assay with A-NE or A-OH and the lysosomal dye reveals that the emissions from adducts of A-NE or A-OH with biothiols are colocalized with those of the lysosomal dye. The high overlap coefficients indicate that A-NE and A-OH can accumulate and react with biothiols in the lysosomes. The stain times show that the process of A-NE is faster than that of A-OH due to the latters need for a longer stain time.

To examine organelle selectivity of these probes for lysosomal thiols, the control assay of cell imaging with a thiol quencher (*N*-ethylmaleimide, NEM) was performed. After incubation with 500 μM for 1 h, the cells were further stained with A-NE or A-OH under the same conditions. No fluorescence was observed from their fluorescence images, as shown in Figure 8i and k.

The cell images of E-OH were observed in our previous communication.[15] A similar result was obtained from cell imaging of E-NE. The cells stained with E-NE emit green fluorescence in almost whole cells, and stronger fluorescence in those regions overlapping with LysoTracker (Figure 8m–p). This may be because the amino is the target group of lysosomes, and E-NE and/or its adduct with biothiols can accumulate to lysosomes to give a stronger emission. Therefore, A-NE and A-OH can sense specifically for biothiols in acidic domains (e.g., lysosomes), and E-NE can react with biothiols in the slightly alkaline cytosol (pH 7.2), resulting in green emission and thereby detecting biothiols in most cellular regions.

Usually, commercial lysosome dyes are chromophores with amino as the target group of lysosomes,[19] which can accumulate to lysosomes. The mechanism of LysoTracker probes has not been firmly established in the memebranes of organelles but is likely to involve protonation and retention. In contrast, QMAs are a class of reaction-type probes, which react with biothiols in the acidic environment of lysosomes, forming Michael adducts with strong fluorescence. QMAs are the first case compounds for labeling lysosomes in a reaction-based sensing mode.

Among these QMAs, A-NE has the largest absorption maximum (480 nm) and can accumulate faster to lysosomes

DOI: 10.1021/acs.joc.5b02041
J. Org. Chem. 2015, 80, 12088–12099

due to its *N*,*N*-diethylamino group, and A-OH with the most suitable pK_{a3} (5.6) can specifically sense biothiols in lysosomes and acidic organelles rather than biothiols in slightly alkaline cytosol. Although its absorption maximum (378 nm) is in the UV region, this shortage can be covered by a two-photon excitation to achieve cell images (Figure S11) for the adduct of A-OH with Cys, possessing strong ICT characteristics.

CONCLUSIONS

A series of 7-substituted 2-(quinolin-2-ylmethylene)malonic acids (QMAs) and their ethyl esters (QMEs) were synthesized, and the pK_a values of QMAs were measured through recording their UV/vis absorption spectra in various pH solutions. As two classes of Michael-type probes for thiols, QMAs and QMEs reveal contrary pH effects on the sensing reaction, i.e., QMAs can sense thiols in acidic solutions (pH < pK_{a3}), and QMEs can react with thiols in alkaline solutions (pH > 7). On the basis of experimental and theoretic studies, it has been demonstrated that the contrary pH effects originate from the activation of two Michael reagents, QMAs and thiols, in two different pH ranges, i.e., QMAs are activated in acidic solutions (pH < pK_{a3}) and neutral RSH ionizes to form more nucleophilic RS^- in alkaline solutions (pH > 7) like most Michael-type probes. The activation of QMAs derives from the intramoleular H-bond between two carboxyl groups, which is assigned to pK_{a3}, i.e., the second carboxyl group. The intramolecular H-bond results in a coplanar conformation between two carboxyl groups and α,β-double bond and thus the strong conjugation between the α,β-unsaturated quinoline moiety and two carboxyl groups. The conjugation enhances C_β electrophilicity of QMAs. Therefore, the sensing behavior of QMAs derives from a novel Michael system, activating QMAs-RSH in acidic solutions (pH < pK_{a3}). Among these QMAs, A-NE and A-OH can act as highly sensitive and selective fluorescent probes for thiols. Furthermore, it was demonstrated that A-NE and A-OH can label lysosomes and other acidic organelles through simultaneous staining of lysosomes by A-NE/A-OH and LysoTracker Red, giving an identical pattern.

EXPERIMENTAL SECTION

Materials and Methods. Unless stated otherwise, all chemical regents were purchased from commercial sources and used without further purification. Solvents of technical quality were distilled prior to use. Water for preparation of solutions was purified with a Millipore water system. MDA-MB 231 cells were purchased from American Type Culture Collection (ATCC). ^{1}H and ^{13}C NMR spectra were recorded on a NMR spectrometer operating at 400 or 300 and 75 MHz, respectively. FT-IR spectra were carried out with an infrared spectrometer. High-resolution mass spectrometry data were obtained with an FTMS spectrometer or an LC-TOF MS spectrometer. UV/vis absorption spectra and fluorescence spectra were recorded at room temperature on a UV/vis spectrometer and sprectrofluorophotometer, respectively.

Measurement of pK_a. The spectral measurements for obtaining pK_a values were performed in various aqueous solutions, which were DMSO/water (4:96 v/v) solvent mixtures with four buffers over a pH range of 2−11, involving 0.1 M citric acid/0.1 M disodium hydrogen phosphate buffer at pH 2−5, a 0.1 M HAc/0.1 M NaAc buffer at pH 5−5.5, 0.1 M Na_2HPO_4/0.1 M NaH_2PO_4 at pH 6−8, and a 0.1 M K_2CO_3/0.1 M $NaHCO_3$ buffer at pH > 8. Water for sample preparation was purified with a Millipore water system. All pH values of solutions were further measured with an MQK-PHS-3C pH meter.

Measurement of Rate Constants. Time-dependent response of QMA to different excess thiols exhibits pseudo-first-order reaction conditions. The rate constant k_{obs} is obtained according to the equation

$$\ln[(A - A_{min})/(A_0 - A_{min})] = -k_{obs}t$$

where A_0, A, and A_{min} are absorption values at certain wavelengths, where thiols have no absorption, of the solution before and after the addition of thiols, and the corresponding adduct or after complete reaction of probe molecules, respectively. Furthermore, a second-order rate constant k_2 was obtained according to the equation, $k_{obs} = k_2[RSH]$, where [RSH] is the concentration of thiols.

Computational Details. All electronic structure optimization and frequency calculations were carried out using the Gaussian 09 program suite.[20] The gas phase geometries of all compounds were optimized with the B3LYP density function at the 6-31+G(d) level without any structural constraints. Harmonic force constants were computed at the optimized geometries to characterize the stationary points as minima or saddle points. For compounds with multiple conformations, efforts were made to find the lowest energy conformation by comparing the structures optimized from different starting geometries. The electrostatic potential maps were drawn based on the optimized structures with the B3LYP density functional at the 6-31+G(d) level.

Cell Culture and MTT Assays. MDA-MB 231 cells were seeded in DMEM (Dulbecco's modified Eagle's medium) supplemented with 10% FBS (fetal bovine serum) in an atmosphere of 5% CO_2 and 95% air at 37 °C. Before the experiment, the cells well placed in a 96-well plate followed by the addition of various concentrations of probes. The final concentrations of probes varied from 0 to 50 μM (0, 10, 20, 30, 40, and 50 μM). The cells were then incubated at 37 °C in an atmosphere of 5% CO_2 and 95% air for 24 h, followed by MTT assays (n = 4).

Cell Imaging Experiments. MDA-MB 231 cells cultured under the conditions described above were employed for cell imaging experiments. The imaging of MDA-MB 231 cells was performed by a laser scanning confocal fluorescence microscope (Zeiss LSM 510 Meta NLO). One group of cells was treated initially with 20 μM A-NE or 20 μM E-NE for 1 h or 20 μM A-OH for 3 h and then stained with 75 nM LysoTracker Red for 0.5 h. Another group of cells was treated initially with 500 μM NEM for 1 h and then 20 μM A-NE for 1 h or 20 μM A-OH for 3 h. The excitation wavelength was 458 nm for A-NE and E-NE, 530 nm for LysoTracker Red for one-photon assays, and 750 nm for A-OH for two-photon assays. Fluorescence signals were collected from the green channel (500−600 nm for A-NE and A-OH, 450−550 nm for E-NE) and the red channel (600−750 nm).

Synthesis and Characterization Data of Related Compounds. *2-Methyl-7-nitroquinoline (**1a**).*[21] 3-Nitroaniline (20.0 g, 145 mmol) was added to a 250 mL two-necked round-bottom flask fitted with a condenser. Hydrochloric acid (5 M, 100 mL) was added, and the mixture was heated to 110 °C. Crotonaldehyde (12.22 g, 174 mmol) was then added as a solution in toluene (10 mL) over a period of 1 h. Upon complete addition of the aldehyde, the reaction was heated for another 1 h, and the solution was allowed to cool to 60 °C. After cooling, the solution was neutralized to pH 7−8. The solution was then extracted with ethyl acetate (3 × 50 mL). The combined organics were dried over $MgSO_4$, filtered, and evaporated under reduced pressure. The resulting solid was purified by silica gel column chromatography (hexane/ethyl acetate, 10:1), affording **1a** as a white solid (2.7 g, 10%). ^{1}H NMR (400 MHz, $CDCl_3$, 25 °C, TMS) δ 9.02 (s, 1H), 8.30 (dd, J_1 = 1.9, J_2 = 8.9 Hz, 1H), 8.20 (d, J = 8.5 Hz, 1H), 7.95 (d, J = 8.9 Hz, 1H), 7.50 (d, J = 8.5 Hz, 1H), 2.86 (s, 3H, CH_3).

*2-Methylquinolin-7-amine (**1d′**).*[22] A stirred cloudy solution of **1a** (560 mg, 1.88 mmol) in ethanol (20 mL) was added dropwise to a solution of $SnCl_2{\cdot}2H_2O$ (2.708 g, 12 mmol) in concentrated hydrochloric acid (4 mL) at room temperature for 15 min. The reaction was quenched with aqueous 10% Na_2CO_3 and filtered. After being washed with water (3 × 10 mL), the residue was dried in vacuo to afford 2-methylquinolin-7-amine (350 mg, 75%) without further purification. ^{1}H NMR (400 MHz, $CDCl_3$, 25 °C, TMS) δ 7.86 (d, J = 8.2 Hz, 1H), 7.55 (d, J = 8.6 Hz, 1H), 7.15 (s, 1H), 7.02 (d, J = 8.2 Hz, 1H), 6.90 (m, 1H), 4.04 (br, 2H, NH_2), 2.67 (s, 3H, CH_3).

DOI: 10.1021/acs.joc.5b02041
J. Org. Chem. 2015, 80, 12088−12099

*N,N-Diethyl-2-methylquinolin-7-amine (**1d**).* Ethyl iodide (1.385 g, 8.88 mmol), **1d′** (333 g, 2.22 mmol), sodium carbonate (1.17 g,11.1 mmol), and *N,N*-dimethylacetamide (20 mL) were mixed and stirred for 7 h at 80 °C. The reaction mixture was poured into water and extracted with ethyl acetate. The organic layer was separated, and the solvent was removed under reduced pressure. The resulting solid was purified by silica gel column chromatography (hexane/ethyl acetate, 10:1), affording compound **1d** (300 mg, 67%) as a brown liquid. R_f = 0.35 (ethyl acetate/petroleum ether, 1:4); ^{1}H NMR (400 MHz, $CDCl_3$, 25 °C, TMS) δ 7.82 (d, J = 8.2 Hz, 1H), 7.56 (d, J = 9.0 Hz, 1H), 7.07 (d, J = 2.2 Hz, 1H), 7.03 (dd, J_1 = 2.6, J_2 = 9.0 Hz, 1H), 6.94 (d, J = 8.2 Hz, 1H), 3.48 (q, J = 7.1 Hz, 4H, CH_2CH_3), 2.66 (s, 3H, CH_3), 1.23 (t, J = 7.1 Hz, 6H, CH_2CH_3); ^{13}C NMR (100 MHz, $CDCl_3$, 25 °C, TMS) δ 158.9, 150.0, 148.7, 135.5, 128.2, 118.6, 117.4, 114.8, 105.3, 44.6, 25.3, 12.7; IR (KBr) νbar 1619, 1512, 1460, 1396, 1356, 1249 cm^{-1}; TOFMS (ESI) calcd for $C_{14}H_{19}N_2$ 215.1548 $[M + H]^+$, found 215.1545.

*7-(Diethylamino)quinoline-2-carbaldehyde (**2d**).* Compound **1** (300 mg, 1.4 mmol) was dissolved in 2 mL of dioxane and then added to 3 mL of dioxane suspension with SeO_2 (0.2 g, 1.8 mmol). The mixture was reacted at 60 °C for 6 h under N_2 atmosphere, and 30 mL of ethyl acetate was added for dilution followed by washing once with water. Solvents were removed in vacuo, and purification by column chromatography (ethyl acetate/petroleum ether, 1:20) gave **2d** (0.24 g, 75%) as a brown liquid. R_f = 0.62 (ethyl acetate/petroleum ether, 1:6); ^{1}H NMR (400 MHz, $CDCl_3$, 25 °C, TMS) δ 10.18 (s, 1H, CHO), 8.08 (d,J = 8.2 Hz, 1H), 7.70 (m, 2H), 7.24 (m, 2H), 3.53 (q, J = 7.1 Hz, 4H, CH_2CH_3), 1.28 (t, J = 7.1 Hz, 6H, CH_2CH_3); ^{13}C NMR (100 MHz, $CDCl_3$, 25 °C, TMS) δ 194.3, 152.8, 150.3, 149.3, 136.5, 128.6, 122.4, 118.5, 113.1, 105.7, 44.7, 12.6; IR (KBr) νbar 1705, 1617, 1506, 1460, 1398, 1355, 1186 cm^{-1}; TOFMS (ESI) calcd for $C_{14}H_{17}N_2O$ 229.1341 $[M + H]^+$, found 229.1348.

2-((7-(Diethylamino)quinolin-2-yl)methylene)malonic acid (A-NE). Compound **2d** (0.12 g, 0.5 mmol) was added to the solution of malonic acid (54 mg, 0.5 mmol) in ethanol (4 mL) and stirred at 50 °C for 30 min in the presence of a catalytic amount (10 mol %) of piperidine under N_2 atmosphere. The precipitate was filtered, washed three times with ethanol (3 × 5 mL), and dried to give A-NE (0.08 g, 50%) as a purple powder. Mp 182−184 °C; ^{1}H NMR (400 MHz, DMSO-d_6, 25 °C, TMS) δ 15.7 (br, COOH), 8.46 (d, J = 8.1 Hz, 1H), 7.91 (m, 2H), 7.63 (d, J = 8.1 Hz, 1H), 7.45 (dd, J_1 = 2.2, J_2 = 9.3 Hz, 1H), 6.76 (d, J = 1.8 Hz, 1H), 3.55 (q, J = 7.0 Hz, 4H, CH_2CH_3), 1.20 (t, J = 7.0 Hz, 6H, CH_2CH_3); ^{13}C NMR (100 MHz, DMSO-d_6, 25 °C, TMS) δ 169.0 (COO), 166.4 (COO), 151.0,148.2, 145.3, 140.3, 138.1, 131.8, 129.9, 122.0, 120.3, 119.6, 98.9, 44.7, 12.8; IR (KBr) νbar 3444, 2973, 1714, 1623, 1565, 1506, 1480, 1401, 1350 cm^{-1}; TOFMS (ESI) calcd for $C_{17}H_{17}N_2O_4$ 313.1188 $[M - H]^-$, found 313.1184.

Diethyl 2-((7-(Diethylamino)quinolin-2-yl)methylene)malonate (E-NE). Compound **2d**(0.12 g, 0.5 mmol) was added to the solution of malonic acid diethyl ester (84 mg, 0.5 mmol) in ethanol (4 mL) and stirred at 50 °C overnight in the presence of a catalytic amount (10 mol %) of piperidine under N_2 atmosphere. The solvent in the reaction mixture was removed, and the crude product was subjected to column chromatography (ethyl acetate/petroleum ether, 1:5) to afford E-NE (40 mg, 15%) as a brown tarry liquid. R_f = 0.50 (ethyl acetate/petroleum ether, 1:5); ^{1}H NMR (400 MHz, $CDCl_3$, 25 °C, TMS) δ 7.93 (d, J = 8.0 Hz, 1H), 7.77 (s, 1H, double bond-H), 7.59 (d, J = 9.1 Hz, 1H), 7.15 (m, 2H), 6.97 (s, 1H), 4.47 (q, J = 7.1 Hz, 2H, CH_2CH_3), 4.33 (q, J = 7.1 Hz, 2H, CH_2CH_3), 3.49 (q, J = 7.0 Hz, 4H, CH_2CH_3), 1.36 (m, 6H, CH_2CH_3), 1.24 (t, J = 7.0 Hz, 6H, CH_2CH_3); ^{13}C NMR (100 MHz, $CDCl_3$, 25 °C, TMS) δ 166.7 (COO), 164.2 (COO), 151.1, 150.2, 148.9, 140.8, 135.8, 129.1, 128.2, 120.6, 118.5, 117.3, 105.7, 61.7, 61.3, 44.6, 14.2, 12.6; IR (KBr) vbar 1731, 1616, 1506, 1460, 1397, 1250, 1217 cm^{-1}; TOFMS (ESI) calcd for $C_{21}H_{26}N_2O_4Na$ 393.1790 $[M + Na]^+$, found 393.1792.

*7-Chloro-2-methylquinoline (**1b**).*[21] 3-Chloroaniline (1.27 g, 10 mmol) was added to a 50 mL two-necked round-bottom flask fitted with a condenser and a septum. Aqueous HCl (5 M, 7 mL) was added, and the resulting mixture was heated to 110 °C. Crotonaldehyde (0.84 g, 12 mmol) was then added as a solution in toluene (2 mL) over a period of 0.5 h using a syringe pump. Upon complete addition of the aldehyde, the reaction was heated for another 1 h, and the solution was allowed to cool to 60 °C. To this hot solution was slowly added $ZnCl_2$ (1.36 g, 10 mmol) as a solution in THF/acetone (10 mL, 1:1), causing a precipitate to form. The reaction vessel was then allowed to cool to room temperature and then cooled in an ice bath for 1 h. The solid was filtered and washed with cold aq HCl (5 M, 15 mL), THF (15 mL), isopropyl alcohol (15 mL), and diethyl ether (15 mL). The resulting white solid was dissolved in a mixture of hexane (100 mL) and aqueous ammonia (29%, 50 mL) and stirred until complete dissolution had been achieved. The organic layer was separated, and the aqueous layer was extracted with diethyl ether (3 × 10 mL). The combined organics were dried over $MgSO_4$, filtered, and evaporated under reduced pressure. The resulting solid was purified by silica gel flash column chromatography (hexane/ethyl acetate, 4:1), affording **1b** as a white solid (0.53 g, 30%); ^{1}H NMR (400 MHz, $CDCl_3$, 25 °C, TMS) δ 8.03 (m, 2H), 7.71 (d, J = 8.7 Hz, 1H), 7.44 (dd, J_1 = 8.6, J_2 = 2.0 Hz, 1H), 7.29 (d, J = 8.5 Hz, 1H), 2.75 (s, 3H, CH_3).

*Quinoline-2-carbaldehyde (**2c**).*[23] 2-Methylquinoline (300 mg, 2.1 mmol) was dissolved in 4 mL of dioxane and then added to 6 mL of dioxane suspension with SeO_2 (302 mg, 2.7 mmol). The mixture was reacted at 60 °C for 6 h under N_2 atmosphere, and 30 mL ethyl acetate was added for dilution followed by washing once with water. The solvents were removed in vacuo, and purification by column chromatography (ethyl acetate/petroleum ether, 1:20) gave **2c** (257 mg, 78%) as a white solid. ^{1}H NMR (400 MHz, $CDCl_3$, 25 °C, TMS) δ 10.25 (s, 1H, CHO), 8.33 (d, J = 8.4 Hz, 1H), 8.27 (d, J = 8.5 Hz, 1H), 8.05 (d, J = 8.4 Hz, 1H), 7.92 (d, J = 8.2 Hz, 1H), 7.84 (m, 1H), 7.71 (m, 1H).

*7-Chloroquinoline-2-carbaldehyde (**2b**).*[24] 7-Chloro-2-methylquinoline (250 mg, 1.41 mmol) was dissolved in 2 mL of dioxane and then added to 3 mL of dioxane suspension with SeO_2 (200 mg, 1.8 mmol). The mixture was reacted at 60 °C for 6 h under N_2 atmosphere, and 30 mL of ethyl acetate was added for dilution followed by washing once with water. The solvents were removed in vacuo, and purification by column chromatography (ethyl acetate/petroleum ether, 1:20) gave **2b** (176 mg, 92%) as a yellow solid. ^{1}H NMR (400 MHz, $CDCl_3$, 25 °C, TMS) δ 10.22 (s, 1H, CHO), 8.31 (d, J = 8.4 Hz, 1H), 8.27 (m, 1H), 8.04 (d, J = 8.4 Hz, 1H), 7.86 (d, J = 8.7 Hz, 1H), 7.65 (dd, J_1 = 8.7, J_2 = 2.1 Hz, 1H).

*7-Nitroquinoline-2-carbaldehyde (**2a**).* 2-Methyl-7-nitroquinoline (265 mg, 1.41 mmol) was dissolved in 2 mL of dioxane and then added to 3 mL of dioxane suspension with SeO_2 (200 mg, 1.8 mmol). The mixture was reacted at 60 °C for 6 h under N_2 atmosphere, and 30 mL of ethyl acetate was added for dilution followed by washing once with water. The solvents were removed in vacuo, and purification by column chromatography (ethyl acetate/petroleum ether, 1:5) gave **2a** (245 mg, 86%) as a white solid. ^{1}H NMR (400 MHz, $CDCl_3$, 25 °C, TMS) δ 10.26 (s, 1H, CHO), 9.17 (d, J = 2.2 Hz, 1H), 8.46 (m, 2H), 8.20 (d, J = 8.5 Hz, 1H), 8.09 (d, J = 9 Hz, 1H). ^{13}C NMR (100 MHz, $CDCl_3$, 25 °C, TMS) δ 192.7, 153.2, 147.9, 145.6, 137.3, 133.7, 128.5, 126.9, 122.9, 120.1; IR (KBr) vbar 2118, 1703, 1618, 1467, 1284 cm^{-1}; TOFMS (ESI) calcd for $C_{10}H_6N_2O_3Na$ 225.0276 $[M + Na]^+$, found 225.0278.

Diethyl 2-(Quinolin-2-ylmethylene)malonate (E-H). Quinoline-2-carbaldehyde (250 mg, 1.6 mmol) was added to the solution of malonic acid diethyl ester (255 mg, 1.6 mmol) in ethanol (10 mL) and stirred at 50 °C overnight in the presence of a catalytic amount (10 mol %) of piperidine under N_2 atmosphere. The solvent in the reaction mixture was removed, and the crude product was subjected to column chromatography (ethyl acetate/petroleum ether, 1:5) to afford E-H (202 mg, 42%) as a light yellow powder. R_f = 0.45 (ethyl acetate/petroleum ether, 1:4); mp 65−66 °C; ^{1}H NMR (400 MHz, $CDCl_3$, 25 °C, TMS) δ 8.20 (d, J = 8.4 Hz, 1H), 8.03 (d, J = 8.5 Hz, 1H), 7.85 (s, 1H, double bond-H), 7.81 (d, J = 8.1 Hz, 1H), 7.73 (m, 1H), 7.58 (m, 1H), 7.51 (d, J = 8.4 Hz, 1H), 4.48−4.54 (q, J = 7.2 Hz, 2H, CH_2), 4.33−4.38 (q, J = 7.2 Hz, 2H, CH_2), 1.37 (m, 6H, CH_3); ^{13}C NMR (100 MHz, $CDCl_3$, 25 °C, TMS) δ 166.5 (COO), 163.9 (COO), 151.0, 147.9, 139.4, 136.8, 130.1, 129.9, 128.0, 127.7, 127.5, 122.8, 61.9, 61.4, 14.1; IR (KBr) νbar 1735, 1697, 1427, 1376, 1309, 1276,

DOI: 10.1021/acs.joc.5b02041
J. Org. Chem. 2015, 80, 12088−12099

1251, 1230 cm^{-1}; TOFMS (ESI) calcd for $C_{17}H_{17}NO_4Na$ 322.1055 $[M + Na]^+$, found 322.1050.

Diethyl 2-((7-Chloroquinolin-2-yl)methylene)malonate (E-Cl). 7-Chloroquinoline-2-carbaldehyde (176 mg, 0.9 mmol) was added to the solution of malonic acid diethyl ester (147 mg, 0.9 mmol) in ethanol (8 mL) and stirred at 50 °C overnight in the presence of a catalytic amount (10 mol %) of piperidine under N_2 atmosphere. The solvent in the reaction mixture was removed, and the crude product was subjected to column chromatography (ethyl acetate/petroleum ether, 1:5) to afford E-Cl (184 mg, 60%) as a yellow powder; R_f = 0.42 (ethyl acetate/petroleum ether, 1:4); mp 116−118 °C; ^{1}H NMR (400 MHz, $CDCl_3$, 25 °C, TMS) δ 8.18 (d, J = 8.4 Hz, 1H), 7.99 (d, J = 2 Hz, 1H), 7.80 (s, 1H, double bond-H), 7.75 (d, J = 8.7 Hz, 1H), 7.51 (m, 2H), 4.50 (q, J = 7.2 Hz, 2H, CH_2), 4.35 (q, J = 7.2 Hz, 2H, CH_2), 1.37 (m, 6H, CH_3); ^{13}C NMR (100 MHz, $CDCl_3$, 25 °C, TMS) δ 166.3 (COO), 163.8 (COO), 152.0, 148.1, 138.8, 136.7, 136.1, 130.7, 128.8, 128.7, 128.6, 126.3, 123.1, 62.0, 61.5, 14.2, 14.1; IR (KBr) vbar 1733, 1699, 1591, 1493, 1412, 1377, 1300, 1262, 1230 cm^{-1}; TOFMS (ESI) calcd for $C_{17}H_{16}NO_4ClNa$ 356.0666 $[M + Na]^+$, found 356.0657.

Diethyl 2-((7-Nitroquinolin-2-yl)methylene)malonate (E-NO). 7-Nitroquinoline-2-carbaldehyde (182 mg, 0.9 mmol) was added to the solution of malonic acid diethyl ester (147 mg, 0.9 mmol) in ethanol (8 mL) and stirred at 50 °C overnight in the presence of a catalytic amount (10 mol %) of piperidine under N_2 atmosphere. The solvent in the reaction mixture was removed, and the crude product was subjected to column chromatography (ethyl acetate/petroleum ether, 1:3) to afford E-NO (167 mg, 54%) as a light yellow powder. R_f = 0.24 (ethyl acetate/petroleum ether, 1:5); mp 126−128 °C; ^{1}H NMR (400 MHz, $CDCl_3$, 25 °C, TMS) δ 8.87 (d, J = 2.2 Hz, 1H), 8.35 (dd, J_1 = 2.2, J_2 = 9 Hz, 1H), 8.30 (d, J = 8.5 Hz, 1H), 7.99 (d, J = 9 Hz, 1H), 7.83 (s, 1H, double bond-H), 7.67 (d, J = 8.5 Hz, 1H), 4.54 (q, J = 7.2 Hz, 2H, CH_2), 4.37 (q, J = 7.2 Hz, 2H, CH_2), 1.39 (m, 6H, CH_3); ^{13}C NMR (100 MHz, $CDCl_3$, 25 °C, TMS) δ 166.0 (COO), 163.5 (COO), 153.6, 148.6, 146.7, 137.8, 137.0, 131.8, 130.8, 129.3, 125.8, 125.6, 120.9, 62.2, 61.7, 14.2, 14.1; IR (KBr) vbar 1738, 1699, 1528, 1348, 1303 cm^{-1}; TOFMS (ESI) calcd for $C_{17}H_{16}N_2O_6Na$ 367.0906 $[M + Na]^+$, found 367.0912.

2-(Quinolin-2-ylmethylene)malonic acid (A-H). Diethyl 2-(quinolin-2-ylmethylene)malonate (0.10 g, 0.33 mmol) was added to the solution of potassium hydroxide (75 mg, 1.3 mmol) in ethanol/water (1:2, 3 mL) and stirred at 80 °C for 2 h under N_2 atmosphere. The precipitate was filtered, washed three times with ethanol (3 × 5 mL), and dried to give A-H (50 mg, 62%) as a light yellow solid. Mp 176−179 °C; ^{1}H NMR (400 MHz, DMSO-d_6, 25 °C, TMS) δ 13.3 (br, 2H, COOH), 8.49 (d, J = 11.3 Hz, 1H), 8.03 (d, J = 10.7 Hz, 1H), 7.97 (d, J = 11.2 Hz, 1H), 7.85 (m, 2H), 7.70 (m, 2H); ^{13}C NMR (100 MHz, DMSO-d_6, 25 °C, TMS) δ 167.8 (COO), 165.7 (COO), 152.0, 147.6, 137.5, 137.4, 132.6, 130.8, 129.5, 128.3, 128.1, 128.0, 123.2; IR (KBr) νbar 3437, 3074, 1725, 1601, 1507, 1438, 1389, 1312 cm^{-1}; FTMS (ESI) calcd for $C_{13}H_8NO_4$ 242.0448 $[M - H]^-$, found 242.0451.

2-((7-Chloroquinolin-2-yl)methylene)malonic acid (A-Cl). Diethyl 2-((7-chloroquinolin-2-yl)methylene)malonate (0.10 g, 0.3 mmol) was added to the solution of potassium hydroxide (67 mg, 1.2 mmol) in ethanol/water (1:2, 3 mL) and stirred at 80 °C for 2 h under N_2 atmosphere. The precipitate was filtered, washed three times with ethanol (3 × 5 mL), and dried to give A-Cl (57 mg, 69%) as a yellow solid. Mp 177−178 °C; ^{1}H NMR (400 MHz, DMSO-d_6, 25 °C, TMS) δ 13.2 (br, 2H, COOH), 8.50 (d, J = 8.5 Hz, 1H), 8.07 (d, J = 8.8 Hz, 1H), 7.94 (d, J = 2.2 Hz, 1H), 7.81 (d, J = 8.5 Hz, 1H), 7.70 (m, 2H); ^{13}C NMR (100 MHz, DMSO-d_6, 25 °C, TMS) δ 167.7 (COO), 165.5 (COO), 153.2, 147.8, 137.7, 136.9, 135.2, 133.3, 130.4, 128.6, 127.9, 126.5, 123.6; IR (KBr) vbar 3439, 3080, 1737, 1619, 1500, 1462, 1318, 1265 cm^{-1}; FTMS (ESI) calcd for $C_{12}H_7NO_2Cl$ 232.0160 $[M - CO_2 - H]^-$, found 232.0163.

2-((7-Nitroquinolin-2-yl)methylene)malonic Acid (A-NO). Diethyl 2-((7-nitroquinolin-2-yl)methylene)malonate (0.10 g, 0.29 mmol) was added to the solution of potassium hydroxide (67 mg, 1.2 mmol) in ethanol/water (1:2, 3 mL) and stirred at 80 °C for 2 h under N_2 atmosphere. The precipitate was filtered, washed three times with ethanol (3 × 5 mL), and dried to give A-NO (46 mg, 55%) as a yellow solid. Mp 185−188 °C; ^{1}H NMR (400 MHz, DMSO-d_6, 25 °C, TMS) δ 13.2 (br, 2H, COOH), 8.73 (d, J = 2.1 Hz, 1H), 8.66 (d, J = 8.5 Hz, 1H), 8.38 (dd, J_1 = 2.3, J_2 = 9.0 Hz, 1H), 8.29 (d, J = 9.1 Hz, 1H), 8.00 (d, J = 8.5 Hz, 1H), 7.70 (s, 1H, double bond-H); ^{13}C NMR (100 MHz, DMSO-d_6, 25 °C, TMS) δ 167.8 (COO), 165.5 (COO), 152.9, 148.1, 142.0, 137.5, 137.0, 133.0, 130.5, 125.6, 122.8, 121.3, 116.8; IR (KBr) vbar 3437, 2981, 2109, 1714, 1643, 1612, 1266, 1220 cm^{-1}; FTMS (ESI) calcd for $C_{13}H_7N_2O_6$ 287.0299 $[M - H]^-$, found 287.0301.

■ ASSOCIATED CONTENT

Supporting Information

The Supporting Information is available free of charge on the ACS Publications website at DOI: 10.1021/acs.joc.5b02041.

Photograph for the color change and fluorescence of A-NE in solutions in the range of pH 2−11 with and without Cys; UV/vis absorption spectra of A-NE and A-OH in different pH solutions; mass spectrum and partial ^{1}H NMR spectra of A-NE/Cys; UV/vis absorption and fluorescence spectra of QMAs in A[-H^+]$^-$ ionized states; photostability and cytotoxicity of A-NE and A-OH; confocal fluorescence image of the MDA-MB 231 cells; atom coordinates and absolute energies for structures of various A-OH ions and E-OH; and copies of NMR spectra of related compounds (PDF)

■ AUTHOR INFORMATION

Corresponding Author

*E-mail: qhsong@ustc.edu.cn.

Notes

The authors declare no competing financial interest.

■ ACKNOWLEDGMENTS

This work was supported by the National Natural Science Foundation of China (Grant 21272224).

■ REFERENCES

(1) (a) Zhang, S.-Y.; Ong, C.-N.; Shen, H.-M. *Cancer Lett.* **2004**, *208*, 143−153. (b) Ball, R. O.; Courtney-Martin, G.; Pencharz, P. B. *J. Nutr.* **2006**, *136*, 1682S−1693S. (c) Hong, R.; Han, G.; Fernández, J. M.; Kim, B.-J.; Forbes, N. S.; Rotello, V. M. *J. Am. Chem. Soc.* **2006**, *128*, 1078−1079. (d) Jensen, K. S.; Hansen, R. E.; Winther, J. R. *Antioxid. Redox Signaling* **2009**, *11*, 1047−1058.

(2) Shahrokhian, S. *Anal. Chem.* **2001**, *73*, 5972−5978.

(3) (a) Refsum, H.; Ueland, P. M.; Nygard, O.; Vollset, S. E. *Annu. Rev. Med.* **1998**, *49*, 31−62. (b) Seshadri, S.; Beiser, A.; Selhub, J.; Jacques, P. F.; Rosenberg, I. H.; D'Agostino, R. B.; Wilson, P. W. F.; Wolf, P. A. *N. Engl. J. Med.* **2002**, *346*, 476−483. (c) van Meurs, J. B. J.; Dhonukshe-Rutten, R. A. M.; Pluijm, S. M. F.; van der Klift, M.; de Jonge, R.; Lindemans, J.; de Groot, L. C. P. G. M.; Hofman, A.; Witteman, J. C. M.; van Leeuwen, J. P. T. M.; Breteler, M. M. B.; Lips, P.; Pols, H. A. P.; Uitterlinden, A. G. *N. Engl. J. Med.* **2004**, *350*, 2033−2041.

(4) (a) Wu, G.; Fang, Y.-Z.; Yang, S.; Lupton, J. R.; Turner, N. D. *J. Nutr.* **2004**, *134*, 489−492. (b) Dalton, T. P.; Shertzer, H. G.; Puga, A. *Annu. Rev. Pharmacol. Toxicol.* **1999**, *39*, 67−101. (c) Kanzok, S. M.; Schirmer, R. H.; Türbachova, I.; Iozef, R.; Becker, K. *J. Biol. Chem.* **2000**, *275*, 40180−40186.

(5) (a) Chen, X.; Zhou, Y.; Peng, X.; Yoon, J. *Chem. Soc. Rev.* **2010**, *39*, 2120−2135. (b) Moragues, M. E.; Martínez-Máñez, R.; Sancenón, F. *Chem. Soc. Rev.* **2011**, *40*, 2593−2643. (c) Kaur, K.; Saini, R.; Kumar, A.; Luxami, V.; Kaur, N.; Singh, P.; Kumar, S. *Coord. Chem. Rev.* **2012**, *256*, 1992−2028. (d) Hyman, L. M.; Franz, K. J. *Coord. Chem. Rev.* **2012**, *256*, 2333−2356. (e) Jung, H. S.; Chen, X.-Q.; Kim,

DOI: 10.1021/acs.joc.5b02041
J. Org. Chem. 2015, 80, 12088−12099

J. S.; Yoon, J. *Chem. Soc. Rev.* **2013**, *42*, 6019−6031. (f) Yin, C.; Huo, F.; Zhang, J.; Martínez-Máñez, R.; Yang, Y.; Lv, H.; Li, S. *Chem. Soc. Rev.* **2013**, *42*, 6032−6059. (g) Manjare, S. T.; Kim, Y.; Churchill, D. G. *Acc. Chem. Res.* **2014**, *47*, 2985−2998. (h) Guo, Z.; Park, S.; Yoon, J.; Shin, I. *Chem. Soc. Rev.* **2014**, *43*, 16−29. (i) Kaur, M.; Choi, D. H. *Chem. Soc. Rev.* **2015**, *44*, 58−77. (j) Tang, Y.; Lee, D.; Wang, J.; Li, G.; Yu, J.; Lin, W.; Yoon, J. *Chem. Soc. Rev.* **2015**, *44*, 5003−5015 and references cited therein..

(6) (a) Stanley, M.; Han, C.; Knebel, A.; Murphy, P.; Shpiro, N.; Virdee, S. *ACS Chem. Biol.* **2015**, *10*, 1542−1554. (b) Freimuth, L.; Christoffers, J. *Chem. - Eur. J.* **2015**, *21*, 8214−8221. (c) Ren, W.-X.; Han, J.-Y.; Pradhan, T.; Lim, J.-Y.; Lee, J.-H.; Lee, J.; Kim, J.-H.; Kim, J.-S. *Biomaterials* **2014**, *35*, 4157−4167. (d) Krishnan, S.; Miller, R. M.; Tian, B.-X.; Mullins, R. D.; Jacobson, M. P.; Taunton, J. *J. Am. Chem. Soc.* **2014**, *136*, 12624−12630. (e) Işık, M.; Guliyev, R.; Kolemen, S.; Altay, Y.; Senturk, B.; Tekinay, T.; Akkaya, E. U. *Org. Lett.* **2014**, *16*, 3260−3263. (f) Lou, X.-D.; Zhao, Z.-J.; Hong, Y.-N.; Dong, C.; Min, X.-H.; Zhuang, Y.; Xu, X.-M.; Jia, Y.-M.; Xia, F.; Tang, B.-Z. *Nanoscale* **2014**, *6*, 14691−14696. (g) Lou, X.-D.; Hong, Y.-N.; Chen, S.-J.; Leung, C. W. T.; Zhao, N.; Situ, B.; Lam, J. W. Y.; Tang, B.-Z. *Sci. Rep.* **2014**, *4*, 4272. (h) Yang, Y.-T.; Huo, F.-J.; Yin, C.-X.; Zheng, A.-M.; Chao, J.-B.; Li, Y.-Q.; Nie, Z.-X.; Martínez-Máñez, R.; Liu, D.-S. *Biosens. Bioelectron.* **2013**, *47*, 300−306.

(7) (a) Hammers, M. D.; Pluth, M. D. *Anal. Chem.* **2014**, *86*, 7135−7140. (b) Nawimanage, R. R.; Prasai, B.; Hettiarachchi, S. U.; McCarley, R. L. *Anal. Chem.* **2014**, *86*, 12266−12271. (c) Malwal, S. R.; Labade, A.; Andhalkar, A. S.; Sengupta, K.; Chakrapani, H. *Chem. Commun.* **2014**, *50*, 11533−11535. (d) Li, M.; Wu, X.-M.; Wang, Y.; Li, Y.-S.; Zhu, W.-H.; James, T. D. *Chem. Commun.* **2014**, *50*, 1751−1753. (e) Liu, J.; Sun, Y.-Q.; Huo, Y.-Y.; Zhang, H.-X.; Wang, L.-F.; Zhang, P.; Song, D.; Shi, Y.-W.; Guo, W. *J. Am. Chem. Soc.* **2014**, *136*, 574−577. (f) Wang, F.-Y.; Guo, Z.-Q.; Li, X.; Li, X.-A.; Zhao, C.-C. *Chem. - Eur. J.* **2014**, *20*, 11471−11478. (g) Lim, S.-Y.; Hong, K.-H.; Kim, D. I.; Kwon, H.; Kim, H.-J. *J. Am. Chem. Soc.* **2014**, *136*, 7018−7025. (h) Huang, C.-S.; Yin, Q.; Meng, J.-J.; Zhu, W.-P.; Yang, Y.; Qian, X.-H.; Xu, Y.-F. *Chem. - Eur. J.* **2013**, *19*, 7739−7747. (i) Fu, N.; Su, D.; Cort, J. R.; Chen, B.-W.; Xiong, Y.-J.; Qian, W.-J.; Konopka, A. E.; Bigelow, D. J.; Squier, T. C. *J. Am. Chem. Soc.* **2013**, *135*, 3567−3575. (j) Niu, L.-Y.; Guan, Y.-S.; Chen, Y.-Z.; Wu, L.-Z.; Tung, C.-H.; Yang, Q.-Z. *Chem. Commun.* **2013**, *49*, 1294−1296.

(8) (a) Rong, L.; Zhang, C.; Lei, Q.; Sun, H.-L.; Qin, S.-Y.; Feng, J.; Zhang, X.-Z. *Chem. Commun.* **2015**, *51*, 388−390. (b) Guo, Y.-S.; Liu, J.; Yang, G.-X.; Sun, X.-F.; Chen, H.-Y.; Xu, J.-J. *Chem. Commun.* **2015**, *51*, 862−865. (c) Li, J.; Tian, C.-C.; Yuan, Y.; Yang, Z.; Yin, C.; Jiang, R.-C.; Song, W.-L.; Li, X.; Lu, X.-M.; Zhang, L.; Fan, Q.-L.; Huang, W. *Macromolecules* **2015**, *48*, 1017−1025. (d) Yuan, Y.-Y.; Kwok, R. T. K.; Feng, G.-X.; Liang, J.; Geng, J.-L.; Tang, B.-Z.; Liu, B. *Chem. Commun.* **2014**, *50*, 295−297. (e) Jung, D.-B.; Maiti, S.; Lee, J. H.; Lee, J. H.; Kim, J. S. *Chem. Commun.* **2014**, *50*, 3044−3047. (f) Lin, Q.-N.; Du, Z.-M.; Yang, Y.-L.; Fang, Q.; Bao, C.-Y.; Yang, Y.; Zhu, L.-Y. *Chem. - Eur. J.* **2014**, *20*, 16314−16319. (g) Ang, C. Y.; Tan, S.-Y.; Lu, Y.-P.; Bai, L.-Y.; Li, M.-H.; Li, P.-Z.; Zhang, Q.; Selvan, S. T.; Zhao, Y.-L. *Sci. Rep.* **2014**, *4*, 7057. (h) Golub, E.; Freeman, R.; Willner, I. *Anal. Chem.* **2013**, *85*, 12126−12133. (i) Lou, Z.-R.; Li, P.; Sun, X.-F.; Yang, S.-Q.; Wang, B.-S.; Han, K.-L. *Chem. Commun.* **2013**, *49*, 391−393.

(9) (a) Mandani, S.; Sharma, B.; Dey, D.; Sarma, T. K. *Nanoscale* **2015**, *7*, 1802−1808. (b) Zhang, P.-Y.; Wang, J.-Q.; Huang, H.-Y.; Chen, H.-M.; Guan, R.-L.; Chen, Y.; Ji, L.-N.; Chao, H. *Biomaterials* **2014**, *35*, 9003−9011. (c) Reddy, G. U.; Agarwalla, H.; Taye, N.; Ghorai, S.; Chattopadhyay, S.; Das, A. *Chem. Commun.* **2014**, *50*, 9899−9902. (d) Altmann, L.; Kunz, S.; Bäumer, M. *J. Phys. Chem. C* **2014**, *118*, 8925−8932. (e) Yuan, X.; Tay, Y.-Q.; Dou, X.-Y.; Luo, Z.-T.; Leong, D. T.; Xie, J.-P. *Anal. Chem.* **2013**, *85*, 1913−1919. (f) Saha, A.; Jana, N. R. *Anal. Chem.* **2013**, *85*, 9221−9228. (g) Zou, T.-T.; Lum, C. T.; Chui, S. S.; Che, C.-M. *Angew. Chem.* **2013**, *125*, 3002−3005. (h) Li, J.-P.; Yang, S.; Zhou, W.-Y.; Liu, C.-H.; Jia, Y.-H.; Zheng, J.; Li, Y.-H.; Li, J.-S.; Yang, R.-H. *Chem. Commun.* **2013**, *49*, 7932−7934. (i) Reboucas, J. S.; James, B. R. *Inorg. Chem.* **2013**, *52*, 1084−1098. (j) Peng, R.-X.; Lin, L.-L.; Wu, X.-X.; Liu, X.-H.; Feng, X.-M. *J. Org. Chem.* **2013**, *78*, 11602−11605.

(10) (a) Zhang, H.-T.; Zhang, C.-Y.; Liu, R.-C.; Yi, L.; Sun, H.-Y. *Chem. Commun.* **2015**, *51*, 2029−2032. (b) Wang, F.-Y.; Zhou, L.; Zhao, C.-C.; Wang, R.; Fei, Q.; Luo, S.-H.; Guo, Z.-Q.; Tian, H.; Zhu, W.-H. *Chem. Sci.* **2015**, *6*, 2584−2589. (c) Yang, X. F.; Huang, Q.; Zhong, Y.; Li, Z.; Li, H.; Lowry, M.; Escobedo, J. O.; Strongin, R. M. *Chem. Sci.* **2014**, *5*, 2177−2183.

(11) (a) Wang, S.-Q.; Wu, Q.-H.; Wang, H.-Y.; Zheng, X.-X.; Shen, S.-L.; Zhang, Y.-R.; Miao, J.-Y.; Zhao, B.-X. *Biosens. Bioelectron.* **2014**, *55*, 386−390. (b) Zhang, Q.; Yu, D.-H.; Ding, S.-S.; Feng, G.-Q. *Chem. Commun.* **2014**, *50*, 14002−14005. (c) Zhang, Y.; Wang, J.-H.; Zheng, W.-J.; Chen, T.-F.; Tong, Q.-X.; Li, D. *J. Mater. Chem. B* **2014**, *2*, 4159−4166. (d) Xiong, X.-Q.; Song, F.-L.; Chen, G.-W.; Sun, W.; Wang, J.-Y.; Gao, P.; Zhang, Y.-K.; Qiao, B.; Li, W.-F.; Sun, S.-G.; Fan, J.-L.; Peng, X.-J. *Chem. - Eur. J.* **2013**, *19*, 6538−6545.

(12) (a) Barve, A.; Lowry, M.; Escobedo, J. O.; Huynh, K. T.; Hakuna, L.; Strongin, R. M. *Chem. Commun.* **2014**, *50*, 8219−8222. (b) Madhu, S.; Gonnade, R.; Ravikanth, M. *J. Org. Chem.* **2013**, *78*, 5056−5060. (c) Mei, J.; Wang, Y.-J.; Tong, J.-Q.; Wang, J.; Qin, A.-J.; Sun, J.-Z.; Tang, B.-Z. *Chem. - Eur. J.* **2013**, *19*, 613−620.

(13) (a) Peng, H.; Wang, K.; Dai, C.; Williamson, S.; Wang, B. *Chem. Commun.* **2014**, *50*, 13668−13671. (b) Li, G.-Y.; Chen, Y.; Wu, J.-H.; Ji, L.-N; Chao, H. *Chem. Commun.* **2013**, *49*, 2040−2042.

(14) (a) Zhao, W.; Liu, W.; Ge, J.; Wu, J.; Zhang, W.; Meng, X.; Wang, P. *J. Mater. Chem.* **2011**, *21*, 13561−13568. (b) Nielsen, J. W.; Jensen, K. S.; Hansen, R. E.; Gotfredsen, C. H.; Winther, J. R. *Anal. Biochem.* **2012**, *421*, 115−120.

(15) Song, Q.-H.; Wu, Q.-Q.; Liu, C.-H.; Du, X.-J.; Guo, Q.-X. *J. Mater. Chem. B* **2013**, *1*, 438−442.

(16) Wu, Q.-Q.; Xiao, Z.-F.; Du, X.-J.; Song, Q.-H. *Chem. - Asian J.* **2013**, *8*, 2564−2568.

(17) Demas, J. N.; Crosby, J. A. *J. Phys. Chem.* **1971**, *75*, 991−1024.

(18) Dawson, W. R.; Windsor, M. W. *J. Phys. Chem.* **1968**, *72*, 3251−3260.

(19) Johnson, M. T. Z. *Spence, The molecular probe® handbook: A guide to fluorescent probes and labeling technologies*, 11th ed.; Life Technologies Corporation: USA, 2010; p 516.

(20) Frisch, M. J.; Trucks, G. W.; Schlegel, H. B.; Scuseria, G. E.; Robb, M. A.; Cheeseman, J. R.; Scalmani, G.; Barone, V.; Mennucci, B.;Petersson, G. A.; Nakatsuji, H.; Caricato, M.; Li, X.; Hratchian, H. P.;Izmaylov, A. F.; Bloino, J.; Zheng, G.; Sonnenberg, J. L.; Hada, M.;Ehara, M.; Toyota, K.; Fukuda, R.; Hasegawa, J.; Ishida, M.; Nakajima,T.; Honda, Y.; Kitao, O.; Nakai, H.; Vreven, T.; Montgomery, J. A.;Peralta, J. E.; Ogliaro, F.; Bearpark, M.; Heyd, J. J.; Brothers, E.;Kudin, K. N.; Staroverov, V. N.; Kobayashi, R.; Normand, J.; Raghavachari, K.; Rendell, A.; Burant, J. C.; Iyengar, S. S.; Tomasi, J. *Gaussian 09*, revision A.02; Gaussian, Inc.: Wallingford, CT, 2009.

(21) Sivaprasad, G.; Rajesh, R.; Perumal, P. T. *Tetrahedron Lett.* **2006**, *47*, 1783−1785.

(22) Sinha, B. K.; Philen, R. M.; Sato, R. *J. Med. Chem.* **1977**, *20*, 1528−1531.

(23) Sun, H.; Su, F.-Z.; Ni, J.; Cao, Y.; He, H.-Y.; Fan, K.-N. *Angew. Chem., Int. Ed.* **2009**, *48*, 4390−4393.

(24) Saravanan, M.; Satyanarayana, B.; Reddy, P. *Synth. Commun.* **2013**, *43*, 2050−2056.

DOI: 10.1021/acs.joc.5b02041
J. Org. Chem. 2015, 80, 12088−12099